Local and remote impacts of atmospheric cloud radiative effects onto the eddy-driven jet

O. Watt-Meyer[1], and D. M. W. Frierson[1]

[1]Department of Atmospheric Sciences, University of Washington, Seattle, USA

Corresponding author: Oliver Watt-Meyer (oliverwm@uw.edu)

Key points

- The response of the eddy-driven jet latitude to the inclusion of cloud radiative effects varies widely across models.
- The Hadley cell and subtropical jet response to clouds is the primary control on how each model's eddy-driven jet shifts.
- An important secondary control arises from the local impact of clouds onto the baroclinicity of the midlatitude atmosphere in each model.

Abstract

This study examines the cause of the spread of extratropical circulation responses to the inclusion of atmospheric cloud radiative effects (ACRE) across atmospheric general circulation models. The ensemble of Clouds On-Off Klimate Intercomparison Experiment aquaplanet simulations shows that these responses include both equatorward and poleward shifts of the eddy-driven jet of varying magnitudes. These disparate extratropical responses occur despite the relatively consistent response in the tropics: a heating in the upper troposphere, which leads to a strengthening of the Hadley cell. It is argued that the eddy-driven jet response is a competition between two effects: the local influence of clouds driving shifts of the jet through meridional gradients in ACRE and the remote impact of a strengthened Hadley cell causing an equatorward shift of the eddy-driven jet. Simulations in which cloud radiative effects are separately turned on in the tropics and extratropics demonstrate this explicitly.

Index terms

3305 Climate change and variability

3310 Clouds and cloud feedbacks

3319 General Circulation

3337 Global climate models

1. Introduction

It is being increasingly recognized that there are strong two-way interactions between cloud radiative effects and the large-scale atmospheric circulation [Bony et al., 2015; Ceppi and Hartmann, 2015]. In general circulation models, cloud radiative effects have been shown to have significant impacts on the mean circulation in the tropics, including acting to strengthen the Hadley cell and subtropical jets and modify the position of the Inter-Tropical Convergence Zone [Slingo and Slingo, 1988, 1991; Li et al., 2015; Harrop and Hartmann, 2016]. Clouds also modify the variability of the tropics, from intraseasonal timescales associated with the Madden-Julian Oscillation [Crueger and Stevens, 2015], to the interannual timescales of the El Niño-Southern Oscillation [Rädel et al., 2016]. Cloud radiative effects are also connected with extratropical annular mode variability, as shown both in observations [Li et al., 2014; Li and Thompson, 2016] and in models [Grise and Polvani, 2014; Grise and Medeiros, 2016], and with Hadley cell extent [Tselioudis et al., 2016]. Biases in the surface shortwave cloud radiative forcing have been shown to be connected to biases in the climatological position of the Southern Hemisphere jet latitude [Ceppi et al., 2012] and the double-Intertropical Convergence Zone (ITCZ) problem [Hwang and Frierson, 2013] in coupled climate models. Clouds also play a role in the dynamical response to external forcing such as increased greenhouse gases. For example, cloud radiative effects have been shown to be responsible for half or more of the poleward shift of the eddy-driven jet in response to either uniformly increased sea surface temperatures [Voigt and Shaw, 2015] or

68 increased CO_2 concentrations [Ceppi and Hartmann, 2016] in specified-SST and
69 slab-ocean aquaplanet simulations, respectively.
70
71 The focus of this study is on understanding the impact of cloud radiative effects onto
72 the climatological position of the eddy-driven jet in atmospheric general circulation
73 models (GCMs). The eddy-driven jet is a region of strong westerly zonal wind that
74 extends through the depth of the troposphere, and exists due to the convergence of
75 angular momentum by eddies (that is, the cyclones and anticyclones generated by
76 baroclinic instability) into a region of maximum baroclinicity. The position of the
77 eddy-driven jet is of fundamental importance for surface climate, as it is related to
78 the meridional maximum in cyclone activity and extratropical precipitation [see
79 review, Shaw et al., 2016]. Furthermore, the latitude of the eddy-driven jet is
80 connected to its timescale of variability [Barnes and Hartmann, 2010], which the
81 fluctuation-dissipation theorem suggests is related to the sensitivity of the jet to
82 external forcing such as increased greenhouse gas concentrations [Kidston and
83 Gerber, 2010; but see also Simpson and Polvani, 2016]. Modern climate models are
84 also known to have significant equatorward biases in the position of the eddy-
85 driven jet in the Southern Hemisphere compared to reanalysis [Bracegirdle et al.,
86 2013]. For these reasons, it is important to understand what factors determine the
87 position of the eddy-driven jet in atmospheric models. One such factor is the impact
88 of cloud radiative effects onto the jet.
89

Despite many studies focused on the connections between cloud radiative effects and dynamical processes in the atmosphere, there is no consensus on the impact of clouds onto the climatological position of the eddy-driven jet. Figure 1 shows the response of the zonal-mean zonal wind to the inclusion of cloud radiative effects in eight different atmospheric general circulation models (details on the simulations are given in Section 2). It is evident that the response of the eddy-driven jet widely varies across models, including a strong equatorward shift (CNRM-CM5; Fig. 1a), a poleward shift (MRI-CGCM3; Fig. 1h) and a broadening of the jet (GFDL-AM2.1; Fig. 1d). The fact that cloud radiative effects have such disparate impacts on the climatological position of the eddy-driven jet across models suggest that the degree to which cloud radiative effects amplify the poleward shift of the jet under global warming [Voigt and Shaw, 2015, 2016; Ceppi and Hartmann, 2016] may be model dependent. The goal of this study is to understand the spread of responses of the eddy-driven jet to cloud radiative effects across models. Briefly, it is found that the response can be explained as a result of two competing effects: tropical cloud radiative effects drive a strengthening of the Hadley cell and an equatorward shifted eddy-driven jet, while extratropical cloud radiative effects impact local baroclinicity in such a way as to shift the jet poleward.

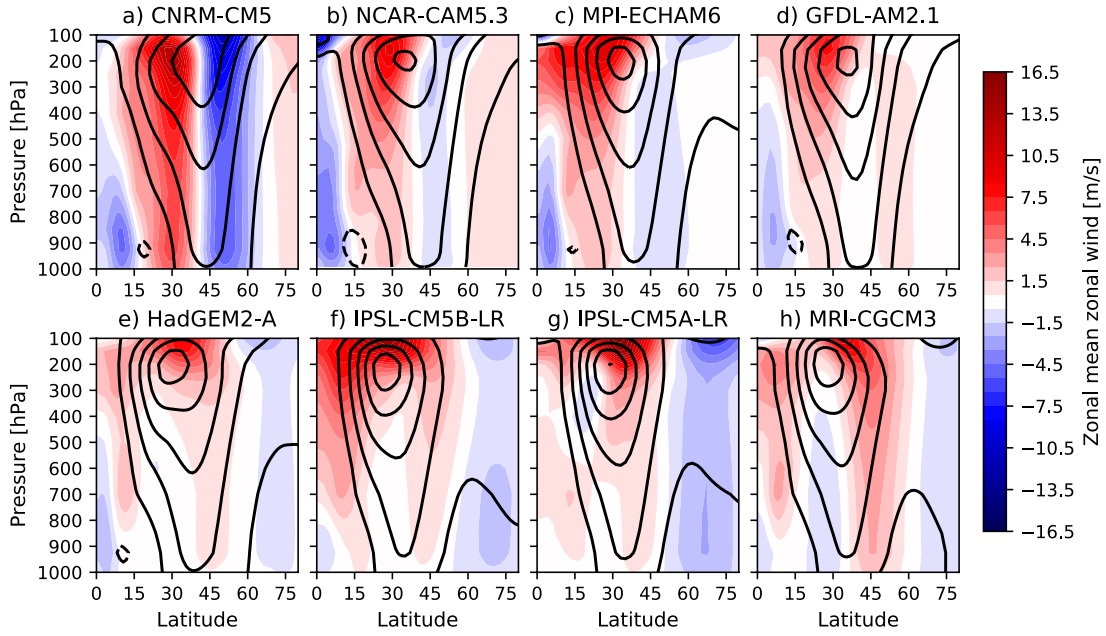

Figure 1: The zonal-mean zonal wind in the clouds off experiment (black contours, 10m/s intervals) and the difference in wind between the clouds on and clouds off experiment (shaded contours) for each model in the COOKIE ensemble.

2. Data and methods

This study uses model output from the Clouds On-Off Klimate Intercomparison Experiment (COOKIE; Stevens et al., 2012), in which simulations are performed with cloud radiative effects turned off ("clouds-off"). That is, the radiative transfer scheme in each model is made to ignore the presence of clouds. These experiments are then compared to control simulations that include cloud radiative effects ("clouds-on"). This experimental procedure, pioneered by Slingo and Slingo (1988), is practical for explicitly identifying the impacts of atmospheric cloud radiative effects onto the modeled circulation. The focus here is on specified-SST aquaplanet simulations, which use the QOBS SST profile and otherwise follow the specifications

123 of the Aqua-Planet Experiment [Neale and Hoskins, 2000]. Using specified-SST
124 aquaplanet experiments eliminates concerns about oceans or land surface warming
125 unrealistically in clouds-off simulations, due to the negative net cloud radiative
126 forcing onto the climate [e.g. Ramanathan et al., 1989]. It also simplifies analysis and
127 interpretation due to the zonal symmetry of the boundary conditions. The COOKIE
128 ensemble includes five models: CNRM [Voldoire et al., 2013], MPI [Stevens et al,
129 2013], HadGEM [Collins et al., 2008], IPSL [Dufresne et al., 2013], and MRI
130 [Yukimoto et al., 2012]. The IPSL model is run with two different physics packages,
131 which are referred to as IPSL-A and IPSL-B, respectively [Hourdin et al, 2013a,b].
132 Each model is run for five years, with no seasonal cycle and perpetual equinoctial
133 solar insolation. In addition to the standard set of COOKIE simulations, additional
134 experiments are performed for this study with the GFDL-AM2.1 [Anderson et al.,
135 2004] and the NCAR-CAM5.3 [Medeiros et al., 2016] models. Standard "clouds-on"
136 and "clouds-off" simulations are performed, with the same specifications as the
137 COOKIE ensemble. The GFDL-AM2.1 experiments are run for 60 years each, while
138 the NCAR-CAM5.3 experiments are run for five years each. As well, experiments are
139 performed with the GFDL and NCAR models in which cloud radiative effects are only
140 turned on in certain latitude bands. Two additional experiments with the GFDL
141 model only turn on cloud radiative effects for the longwave and shortwave bands,
142 respectively. The details of these experiments are described in the Supplementary
143 Information. Because of the hemispheric symmetry of the simulations, Northern and
144 Southern Hemispheres are averaged, but it has been verified that there is no

qualitative change in the results if only the Northern or Southern Hemispheres are used.

The position of the eddy-driven jet is quantified as the latitude of the maximum zonal-mean zonal wind at 850hPa (844hPa and 860hPa for the GFDL AM2.1 and NCAR-CAM5.3 simulations respectively). The latitude is computed by fitting a quadratic polynomial to the grid point of maximum wind and two points on either side [Simpson and Polvani, 2016], and is denoted ϕ_{on} and ϕ_{off} for the clouds-on and clouds-off experiments, respectively. The strength of the Hadley cell is measured as the maximum of the meridional mass streamfunction, and is denoted ψ_{on} and ψ_{off} for the clouds-on and clouds-off experiments, respectively. The difference in the eddy-driven jet latitude and the Hadley cell strength between the clouds-off and the cloud-on simulations are denoted $\Delta\phi = \phi_{on} - \phi_{off}$ and $\Delta\psi = \psi_{on} - \psi_{off}$, respectively. To measure the impact of cloud radiative effects onto the meridional temperature gradient of the atmosphere, the net atmospheric cloud radiative effect (ACRE) is computed. Specifically, using variable names of the CMIP5 convention [Taylor et al., 2012],

$$ACRE = rsus_{cld} - rsut_{cld} - rsds_{cld} - rlds_{cld} - rlut_{cld} \quad (1)$$

where the "cld" subscript represents the difference between total and clear-sky radiative fluxes, i.e.: $rsus_{cld} = rsus - rsuscs$. This quantity is computed for all of the clouds-on experiments, and is also computed for clouds-off experiments for the models that output the necessary data (the ACRE is only computed for diagnostic

purposes in the clouds-off experiments; it is not actually imposed in the model simulations).

Since the meridional position of maximum eddy growth, and thus the position of the eddy-driven jet, tends to be collocated with the maximum absolute temperature gradient [e.g. Lindzen and Farrell, 1980], we compute the meridional gradient of the ACRE as a measure of the impact of clouds onto the temperature gradient of the atmosphere. To quantify how local cloud radiative effects modify the position of the eddy-driven jet, the difference in the meridional gradient of ACRE poleward and equatorward of the jet position is computed as:

$$ACRE\_GRAD\_diff = \text{mean}_{\phi_{off}<\phi<\phi_{off}+\alpha}\left(\frac{1}{a}\partial_\phi ACRE(\phi)\right) - \text{mean}_{\phi_{off}-\alpha<\phi<\phi_{off}}\left(\frac{1}{a}\partial_\phi ACRE(\phi)\right) \quad (2)$$

where α is the latitude range over which the average is taken and a is the radius of the Earth. A range of values of α were tested, and for the results shown in the next section, $\alpha = 10°$ will be used. In the Northern Hemisphere, the climatological meridional gradient of temperature is negative. Thus, when ACRE_GRAD_diff is negative, cloud radiative effects act to increase the absolute value of the gradient poleward of the clouds-off jet position and/or decrease it equatorward of the clouds-off jet position. This indicates that local cloud radiative effects will act to shift the jet poleward when ACRE_GRAD_diff is negative, and equatorward when it is positive.

3. Results

The response of the position of the eddy-driven jet to the inclusion of cloud radiative effects varies widely across models both in magnitude and sign (Fig. 1). In

some models, the jet shifts equatorward (CNRM-CM5, MPI-ECHAM6, NCAR-CAM5.3), in another there is a clear poleward shift (MRI-CGCM3) and in another there is no change in position, but a broadening of the jet (GFDL-AM2.1). Table 1 lists the eddy-driven jet shift for each model. This spread of responses occurs despite a relatively consistent response across the models of a strengthened Hadley cell and equatorward contracted ITCZ (Fig. S2 and see Harrop and Hartmann [2016]), and an accelerated subtropical jet. The strengthened Hadley circulation can be understood as a response to the cloud radiative heating in the tropical upper troposphere (Fig. S3). The heating has a strong meridional gradient, which the Hadley cell responds to by accelerating in order to export more energy from the tropics. This directly leads to a strengthening of the subtropical jet by the transport of westerly angular momentum. The strength of the subtropical jet is known to be related to the position of the eddy-driven jet, with a stronger subtropical jet being associated with an equatorward shifted eddy-driven jet [Lee and Kim, 2003; Ceppi et al., 2013]. There are multiple theories to explain this connection, including the possibility of stronger baroclinicity on the poleward flank of the subtropical jet when it is strong [Lee and Kim, 2003; Brayshaw et al., 2008] or because eddies generated in the mid-latitudes are able to propagate further equatorward with a stronger subtropical jet [Barnes and Hartmann, 2011; Ceppi et al., 2013].

Table 1: The values of the eddy-driven jet latitude in the clouds-off simulation, and its shift ($\Delta\phi$), the Hadley cell strength in the clouds-off simulation, and its shift ($\Delta\psi$) and ACRE_GRAD_diff for each COOKIE simulation. In this table and in all figures, the models are sorted in order of increasing $\Delta\phi$.

Model	**ϕ_{off} [°N]**	**$\Delta\phi$ [° poleward]**	**ψ_{off} [10^9 kg/s]**	**$\Delta\psi$ [10^9 kg/s]**	**ACRE_GRAD_diff [10^{-6} W/m^3]**
CNRM-CM5.1	43.4	-4.70	106.1	53.3	-5.82
NCAR-CAM5.3	42.3	-1.21	135.6	45.0	-7.91
MPI-ECHAM6	38.5	-1.16	180.0	62.5	-8.11
GFDL-AM2.1	39.7	-0.03	160.4	38.7	-8.01
HadGEM2-A	39.1	0.49	219.6	56.6	-16.8
IPSL-CM5B-LR	34.3	0.65	195.5	12.0	-12.0
IPSL-CM5A-LR	34.7	0.85	172.2	-20.5	-17.7
MRI-CGCM3	35.2	1.88	222.4	15.5	-13.8

However, despite the increase in the strength of the Hadley cell in nearly all of the eight models (Fig. S2 and Table 1), there is only a clear equatorward shift of the eddy-driven jet in three models (CNRM-CM5, NCAR-CAM5.3 and MPI-ECHAM6, Figs. 1a-c). This suggests that cloud radiative effects must be affecting the position of the jet through a mechanism beyond their impact on the strength of the Hadley cell. In order to explore this possibility, additional simulations were performed with the GFDL-AM2.1 and NCAR-CAM5.3 models in which cloud radiative effects were only turned on in certain latitude bands (see Supplementary Information). Figure 2 shows the zonal wind response to cloud radiative effects imposed only in the tropics (equatorward of 30°; second column of Fig. 2) and only in the extratropics (poleward of 30°; third column of Fig. 2). In both models, there are opposing impacts from the cloud radiative effects in each region: tropical clouds drive a strong equatorward shift of the jet, consistent with the strengthening of the Hadley

cell (Fig. S4), while clouds in the extratropics shift the eddy-driven jet poleward. When including cloud radiative effects at all latitudes these effects nearly exactly cancel at 850hPa for the GFDL-AM2.1 model while the tropical response is slightly stronger for the NCAR-CAM5.3 model (last column of Fig. 2). This results in no shift of the eddy-driven jet for the GFDL-AM2.1 model, and a moderate equatorward shift for the NCAR-CAM5.3 model for the response to all clouds. These experiments suggest that cloud radiative effects in the tropics and extratropics act as competing influences on the position of the eddy-driven jet.

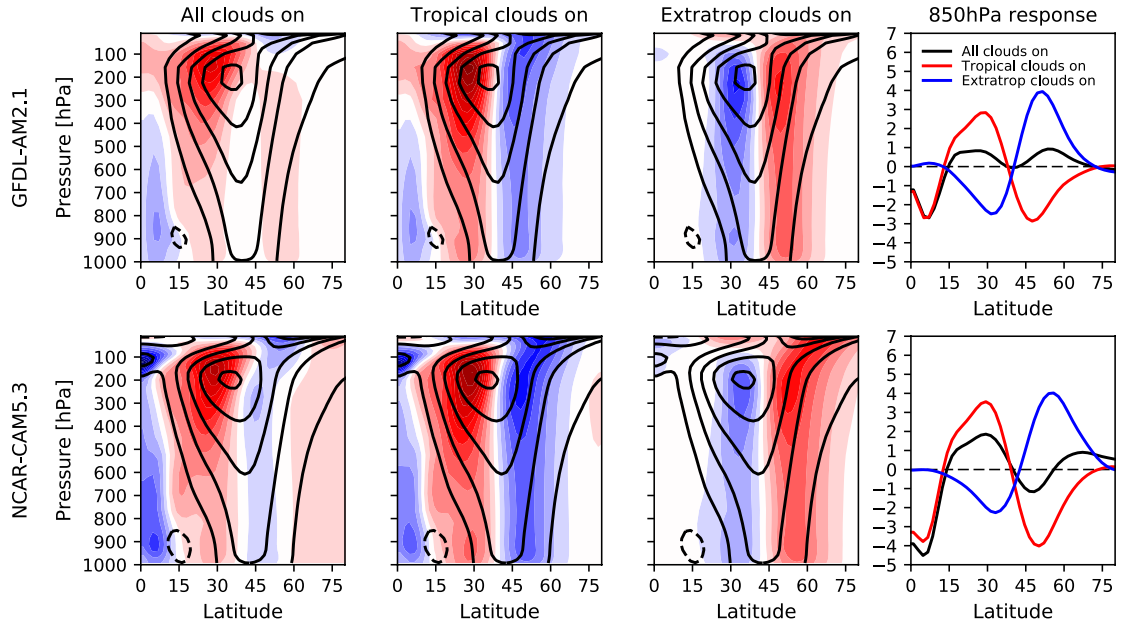

Figure 2: The zonal-mean zonal wind in the GFDL-AM2.1 (top row) and NCAR-CAM5.3 (bottom row) clouds off experiment (black contours, 10m/s intervals) and in the shading the difference in wind between the (first column) all clouds on, (second column) tropical clouds on and (third column) extratropical clouds on and clouds off experiments. The contour interval is 1m/s for the shading, centered about 0, as in Fig. 1. The rightmost column shows the difference in zonal mean zonal wind at 850hPa between clouds on and clouds off for each experiment.

Although it is not possible to perform such an experiment with all of the COOKIE models, the differing impacts of cloud radiative effects in the tropics versus extratropics are captured as follows. The tropical impact is measured by the change in strength of the Hadley cell $\Delta\psi$. The extratropical impact is measured by the difference in ACRE gradient poleward and equatorward of the eddy-driven jet (ACRE_GRAD_diff, see Section 2). Figure 3 shows the ACRE for the clouds-on simulation of each COOKIE model and marks the latitudes of the eddy-driven jet for each simulation. For the models for which data is available, the ACRE for the clouds-off simulations is plotted as well. Although there is general agreement that clouds act to heat the atmospheric column in the tropics and cool in the high latitudes, and that there is a local maximum in ACRE in the mid-latitudes, there are significant differences in the amplitude and detailed structure of ACRE between the models. In particular, the meridional gradient in ACRE (Fig. S5) near the latitude of the eddy-driven jet, which will impact the baroclinicity of the atmosphere and hence the preferred region for eddy-growth and the latitude of the eddy-driven jet, varies strongly between models. Finally, note that outside of the tropics the ACRE in the clouds-off experiments is generally quite similar to the ACRE in the clouds-on experiment. This indicates that, in the extratropics, the feedback of dynamical changes resulting from the inclusion of cloud radiative effects back onto the ACRE is relatively small.

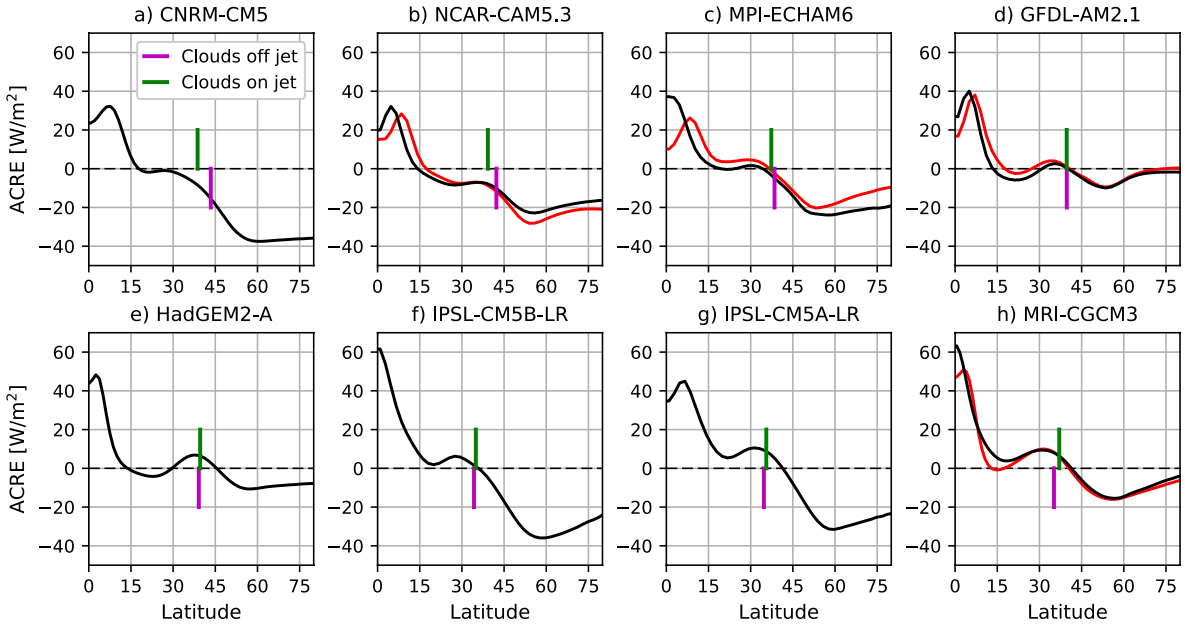

Figure 3: ACRE for the clouds-on simulations of each model, with the latitude of the eddy-driven jet in the clouds off and clouds on simulations marked by vertical magenta and green lines, respectively. The ACRE for the clouds-off simulation (computed only for diagnostic purposes) is shown in red, for the models for which it is available.

To demonstrate the connection between changes in the strength of the Hadley cell, mid-latitude ACRE-gradient and the resulting eddy-driven jet shift, Fig. 4 shows scatter plots between these quantities. Across the eight COOKIE simulations, and the additional eight customized experiments with the GFDL-AM2.1 and NCAR-CAM5.3 models (see Supplementary Information) there is a clear connection between the change in Hadley cell strength $\Delta\psi$ and the jet shift $\Delta\phi$ ($r = -0.65$; Fig. 4a). Although the connection between ACRE_GRAD_diff and $\Delta\phi$ is not as strong ($r = -0.35$; Fig. 4b) it still explains an important part of the variance in the eddy-driven jet shift. For example, focusing on three models with similar positive changes in Hadley cell strength: CNRM-CM5.1, MPI-ECHAM6 and HadGEM2-A, their differing

ACRE_GRAD_diff (see Fig. 4b or Table 1) can at least partially explain their substantially varying responses to the imposition of cloud radiative effects (i.e. a strong equatorward shift, a weak equatorward shift, and a weak poleward shift, respectively). Using a different value of α, which is the latitude range over which ACRE_GRAD_diff is averaged north- and southward of the jet, leads to moderate changes in the correlation computed for Fig. 4b (e.g. $\alpha = 5°$ gives $r = -0.40$, $\alpha = 15°$ gives $r = -0.24$). In order to demonstrate the joint effects of $\Delta\psi$ and ACRE_GRAD_diff onto the jet shift, Fig. 4c shows a scatter plot of these two quantities, with the color and size of the markers representing the sign and magnitude of $\Delta\phi$. Due to the negative correlations between each of these quantities and the jet shift, it is expected that points that fall in the upper-right quadrant will have equatorward shifts, while those in the lower-left quadrant will have poleward shifts. To quantify these connections, a least-squares best fit of the function

$$\Delta\phi = A \cdot \Delta\psi + B \cdot ACRE\_GRAD\_diff + C \quad (3)$$

is made to the data. This plane, using the best fit computed values of A=-0.046° / (10^9 kg/s), B=-0.12° / (10^{-6} W/m^2/m) and C=0.15°, is shown in Fig. 4c. Using this linear regression, the separate impacts of $\Delta\psi$ and ACRE_GRAD_diff can be removed from the data (Figs. S5a-b) and the actual jet shift can be plotted against the predicted jet shift using Eq. 3 (Fig. S6c). Together, the two variables explain 53% of the variance of the eddy-driven jet shift.

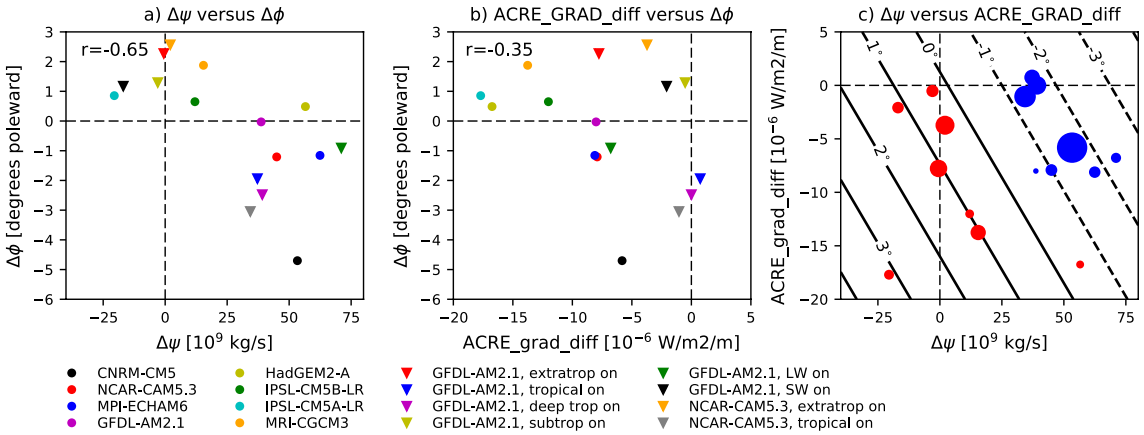

Figure 4: Scatter plots of a) $\Delta\psi$ versus $\Delta\phi$, b) ACRE_GRAD_diff versus $\Delta\phi$, and c) $\Delta\psi$ versus ACRE_GRAD_diff, with the size of markers representing the magnitude of $\Delta\phi$ (red poleward, blue equatorward). In c), the least-squares fit of Eq. 3 to the given data (including all the COOKIE simulations, and the additional GFDL-AM2.1 and NCAR-CAM5.3 experiments) is shown in the solid and dashed contours. Circle markers represent standard COOKIE experiments, while triangles indicate experiments where cloud radiative effects are only imposed in certain regions or for just longwave or shortwave.

Figure S6c also makes it clear that there are two models whose behaviour is furthest from the simple linear relationship: the actual jet shift for both the CNRM-CM5 and IPSL-CM5A-LR models is significantly more equatorward than the predicted shifts. For the CNRM-CM5 model, this may be because the climatological Hadley cell for the clouds-off simulation is the weakest out of all of the considered models and its eddy-driven jet in the clouds-off simulation is the most poleward. Previous research suggests that the eddy-driven jet position is most sensitive to the subtropical jet strength when it is further poleward and the subtropical jet is weaker (see Fig. 3 of Ceppi et al. [2013]). For the IPSL-CM5A-LR model, despite a slight weakening in the

strength of the Hadley cell as measured by the maximum of the streamfunction, there is not a clear weakening of the subtropical jet (Fig. 1g) and this may explain the more moderate poleward shift of the eddy-driven jet than expected from the linear regression.

4. Conclusions and discussion

Atmospheric general circulation models exhibit a wide range of responses of the position of their eddy-driven jet to the inclusion of cloud radiative effects. By separately imposing cloud radiative effects only in the tropics or in the extratropics, it was shown that clouds in each of these regions have opposing impacts on the position of the jet. In the tropics, high clouds warm the upper troposphere in the tropics and consequently accelerate the Hadley cell and thus the subtropical jet. A strengthened subtropical jet tends to lead to an equatorward shifted eddy-driven jet. However, cloud radiative effects in the extratropics also locally affect zonal mean temperature gradients, and act to shift the position of the eddy-driven jet. It is found that clouds have a tendency to increase the temperature gradient on the poleward side of the eddy-driven jet, and hence locally they act to shift the jet poleward. Ultimately, the change in Hadley cell strength and the local impact of cloud radiative effects together are found to explain 53% of the variance across models of the meridional shift of the eddy driven jet.

Given that different atmospheric GCMs, even in a simplified aquaplanet configuration, do not agree on the sign of the eddy-driven jet latitude response to

344 the inclusion of cloud radiative effects, it is necessary to treat with caution results
345 examining the coupling between clouds and the extratropical circulation in only one
346 or two models. Furthermore, because of the strong influence of the tropical
347 circulation onto the extratropics, when examining the possible coupling between
348 cloud radiative effects and circulation in the mid- to high-latitudes, it is necessary to
349 consider the possible effects that cloud radiative effects in the tropics are having
350 onto the higher latitudes.
351
352 Important questions for future work include addressing more precisely why the
353 atmospheric cloud radiative effect is different across models, and why the Hadley
354 cell response differs so strongly between models. To properly address this, the
355 height-dependent cloud heating rates are needed, which are not standard output for
356 COOKIE or CMIP5 experiments. Furthermore, other aspects of the simulations
357 beyond the direct cloud heating could affect the changes in Hadley cell strength,
358 such as the convection scheme or other parameterized processes, or the impacts of
359 tropical variability onto the Hadley circulation. For the extratropics, it is evident
360 from this study that subtle changes in the precise region of cloud heating (and more
361 directly, ACRE gradients) will affect the position of the eddy-driven jet.
362 Furthermore, in the extratropics there are large differences in the cloud heating
363 rates between the boundary layer and the free troposphere (Fig. S3), and the
364 differing impacts of heating in each of these regions of forcing may be important for
365 understanding the response of the eddy-driven jet.
366

This study has focused on specified-SST simulations, which necessarily limit to some extent the response of low clouds to changes in circulation. However, previous studies have emphasized the importance of low cloud changes modifying baroclinicity and hence the eddy-driven jet position [e.g. Ceppi et al., 2012]. Although applying the COOKIE framework in a model with a slab or dynamical ocean is challenging due to the net surface cooling effect of clouds, possible future ways to address this issue would be to apply SST perturbations in a specified-SST model that mimic the low cloud radiative effect [as in Voigt and Shaw, 2016] or to include a Q-flux term such that a clouds-off slab ocean simulation would maintain the same globally averaged surface temperature as a clouds-on one, enabling a more realistic comparison. Finally, future work will also aim to use this study's novel understanding of the local and remote impacts of cloud radiative effects in order to better constrain the spread of eddy-driven jet responses to global warming across models.

Acknowledgements

O. W. was supported by the NOAA Climate and Global Change Postdoctoral Fellowship Program, administered by UCAR's Cooperative Programs for the Advancement of Earth System Science. D. M. W. F. was supported by NSF grants AGS-1359464, PLR-1341497, and AGS-1665247. O. W. thanks P. Ceppi and B. Medeiros for assistance with implementing clouds-off simulations in the GFDL and NCAR models respectively, and B. Harrop for assistance with obtaining COOKIE data.

References

Anderson, J., and Coauthors (2004), The New GFDL Global Atmospheric and Land Model AM2-LM2: Evaluation with prescribed SST simulations, *J. Clim.,* 17, 4641-4673, doi:10.1175/JCLI-3223.1

Barnes, E. A. and D. L. Hartmann (2010), Testing a theory for the effect of latitude on the persistence of eddy-driven jets using CMIP3 simulations, *Geophys. Res. Lett.,* 37, L15801, doi:10.1029/2010GL044144.

Barnes, E. A., and D. L. Hartmann (2011), Rossby wave scales, propagation, and the variability of eddy-driven jets, *J. Atmos. Sci.,* 68, 2893-2908, doi:10.1175/JAS-D-11-039.1.

Bony, S., et al. (2015), Clouds, circulation and climate sensitivity, *Nature Geosci.,* 8, 261-268, doi:10.1038/NGEO2398.

Bracegirdle, T. J., and Coauthors (2013), Assessment of surface winds over the Atlantics, Indian, and Pacific Ocean sectors of the Southern Ocean in CMIP5 models: historical bias, forcing response, and state dependence, *J. Geophys. Res. Atm.,* 118, 547-562, doi:10.1002/jgrd.50153.

Brayshaw, D. J., B. Hoskins and M. Blackburn (2008), The Storm-Track Response to Idealized SST Perturbations in an Aquaplanet GCM, *J. Atmos. Sci.,* 65, 2842-2860, doi:10.1175/2008JAS2657.1.

Ceppi, P., Y.-T. Hwang, D. M. W. Frierson and D. L. Hartmann (2012), Southern Hemisphere jet latitude biases in CMIP5 models linked to shortwave cloud forcing, *Geophys. Res. Lett.,* 39, L19708, doi:10.1029/2012GL053115.

412 Ceppi, P., Y.-T. Hwang, X. Liu, D. M. W. Frierson, and D. L. Hartmann (2013), The
413 relationship between the ITCZ and the Southern Hemispheric eddy-driven jet,
414 *J. Geophys. Res. Atmos.,* 118, 5136-5146, doi:10.1002/jgrd.50461.
415 Ceppi, P., and D. L. Hartmann (2015), Connections Between Clouds, Radiation, and
416 Midlatitude Dynamics: a Review, *Curr. Clim. Change Rep.*, 1: 94,
417 doi:10.1007/s40641-015-0010-x.
418 Ceppi, P., and D. L. Hartmann (2016), Clouds and the Atmospheric Response to
419 Warming, *J. Clim.*, 29, 783-799, doi: 10.1175/JCLI-D-15-0394.1.
420 Collins, W., and Coathors (2008), Evaluation of HadGEM2 model, Met Office Hadley
421 Centre Tech. Note 74, 47 pp.
422 Crueger, T., and B. Stevens (2015), The effect of atmospheric radiative heating by
423 clouds on the Madden-Julian Oscillation, *J. Adv. Model. Earth Syst.,* 7, 854-864,
424 doi:10.1002/2015MS000434.
425 Dufresne, J. L., and Coathors (2013), Climate change projections using the IPSL-CM5
426 Earth System Model: From CMIP3 to CMIP5, *Climate Dyn.*, 40, 2123-2165,
427 doi:10.1007/s00382-012-1636-1.
428 Harrop, B. E., and D. L. Hartmann (2016), The Role of Cloud Radiative Heating in
429 Determining the Location of the ITCZ in Aquaplanet Simulations, *J. Clim.,* 29,
430 2741-2763, doi: 10.1175/JCLI-D-15-0521.1.
431 Hourdin, F., and Coauthors (2013a), Impact of the LMDZ atmospheric grid
432 configuration on the climate and sensitivity of the IPSL-CM5A coupled model,
433 *Climate Dyn.,* 40, 2167-2192, doi:10.1007/s00382-012-1411-3.

Hourdin, F., and Coauthors (2013b), The atmospheric component of the IPSL climate model with revisited parameterizations for clouds and convection, *Climate Dyn.,* 40, 2193-2222, doi:10.1007/s00382-012-1343-y.

Hwang, Y.-T., and D. M. W. Frierson (2013), Link between the double-Intertropical Convergence Zone problem and cloud biases over the Southern Ocean, *Proc. Natl. Acad. Sci. U.S.A.,* 110, 4935-4940, doi: 10.1073/pnas.1213302110.

Kidston, J., and E. P. Gerber (2010), Intermodel variability of the poleward shift of the austral jet stream in the CMIP3 integrations linked to biases in 20th century climatology, *Geophs. Res. Lett.,* 37, L09708, doi:10.1029/2010GL042873.

Lee, S., and H.-K. Kim (2003), The Dynamical Relationship between Subtropical and Eddy-Driven Jets, *J. Atmos. Sci.,* 60, 1490-1503, doi:10.1175/1520-0469(2003)060<1490:TDRBSA>2.0.CO;2.

Li, Y., D. W. J. Thompson, Y. Huang, and M. Zhang (2014), Observed linkages between the northern annular mode/North Atlantic Oscillation, cloud incidence, and cloud radiative forcing, *Geophys. Res. Lett.,* 41, 1681-1688, doi:10.1002/2013GL059113.

Li, Y., D. W. J. Thompson and S. Bony (2015), The Influence of Atmospheric Cloud Radiative Effects on the Large-Scale Atmospheric Circulation, *J. Clim.,* 28, 7263-7278, doi: 10.1175/JCLI-D-14-00825.1.

Li, Y., and D. W. J. Thompson (2016), Observed Signatures of the Barotropic and Baroclinic Annular Modes in Cloud Vertical Structure and Cloud Radiative Effects, *J. Clim.,* 29, 4723-4740, doi:10.1175/JCLI-D-15-0692.1.

456 Lindzen, R. S., and B. Farrell (1980), A Simple Approximate Result for the Maximum
457 Growth Rate of Baroclinic Instabilities, *J. Atmos. Sci.,* 37, 1648-1654, doi:
458 10.1175/1520-0469(1980)037<1648:ASARFT>2.0.CO;2.
459 Medeiros, B., D. L. Williamson, and J. G. Olson (2016), Reference aquaplanet climate
460 in the Community Atmosphere Model, Version 5, *J. Adv. Model. Earth Syst.,* 8,
461 406-424, doi:10.1002/2015MS000593.
462 Neale, R. B., and B. J. Hoskins (2000), A standard test for AGCMs including their
463 physical parameterizations: I: The proposal, *Atmos. Sci. Lett.*, 1, 101-107,
464 doi:10.1006/asle.2000.0022.
465 Rädel, G., and Coauthors (2016), Amplification of El Niño by cloud longwave
466 coupling to atmospheric circulation, *Nature Geosci.,* 9, 106-110, doi:
467 10.1038/NGEO2630.
468 Ramanathan, V., and Coauthors (1989), Cloud-Radiative Forcing and Climate:
469 Results from the Earth Radiation Budget Experiment, *Science,* 243, 57-63,
470 10.1126/science.243.4887.57.
471 Shaw, T. A., and Coauthors (2016), Storm track processes and the opposing
472 influences of climate change, *Nature Geosci.,* 9, 656-665,
473 doi:10.1038/NGEO2783.
474 Simpson, I. R., and L. M. Polvani (2016), Revisiting the relationship between jet
475 position, forced response, and annular mode variability in the southern
476 midlatitudes, *Geophys. Res. Lett.,* 43, 2896-2903, doi:10.1002/2016GL067989.

Slingo, A., and J. M. Slingo (1988), The response of a general circulation model to cloud longwave radiative forcing. I: Introduction and initial experiments, *Q. J. R. Meteorol. Soc.,* 114, 1027-1062, doi: 10.1002/qj.49711448209.

Slingo, J. M., and A. Slingo (1991), The response of a general circulation model to cloud longwave radiative forcing. II: Further studies, *Q. J. R. Meteorol. Soc.,* 117, 333-364, doi: 10.1002/qj.49711749805.

Stevens, B., S. Bony and M. J. Webb (2012), Clouds On-Off Klimate Intercomparison Experiment (COOKIE), available online at: http://hdl.handle.net/11858/00-001M-0000-0024-580A-3.

Stevens, B., and Coauthors (2013), Atmospheric component of the MPI-M Earth system model: ECHAM6, *J. Adv. Model. Earth Syst.,* 5, 146-172, doi:10.1002/jame.20015.

Taylor, K. E., R. J. Stouffer, and G. A. Meehl (2012), An Overview of CMIP5 and the Experiment Design, *Bull. Am. Meteorol. Soc.,* 93, 485-498, doi:10.1175/BAMS-D-11-00094.1.

Tselioudis, G., B. R. Lipat, D. Konsta, K. M. Grise, and L. M. Polvani (2016), Midlatitude cloud shifts, their primary link to the Hadley cell, and their diverse radiative effects, *Geophys. Res. Lett.,* 43, 4594-4601, doi:10.1002/2016GL068242.

Voigt, A., and T. A. Shaw (2015), Circulation response to warming shaped by radiative changes of clouds and water vapour, *Nature Geosci.*, 8, 102-106, doi:10.1038/NGEO2345.

499 Voigt, A., and T. A. Shaw (2016), Impact of Regional Atmospheric Cloud Radiative
500 Changes on Shifts of the Extratropical Jet Stream in Response to Global
501 Warming, *J. Clim.*, 29, 8399-8421, doi: 10.1175/JCLI-D-16-0140.1.
502 Yukimoto, S., and Coauthors (2012), A new global climate model of the
503 Meteorological Research Institute: MRI-CGCM3: Model description and basic
504 performance, *J. Meteor. Soc. Japan*, 90A, 23-64, doi:10.2151/jmsj.2012-A02.